Cell, Vol. 107, 537–548, November 16, 2001, Copyright ©2001 by Cell Press

Mus81-Eme1 Are Essential Components of a Holliday Junction Resolvase

Michael N. Boddy,[1,4] Pierre-Henri L. Gaillard,[1,4] W. Hayes McDonald,[2] Paul Shanahan,[1] John R. Yates 3rd,[2] and Paul Russell[1,2,3]

[1] Department of Molecular Biology
[2] Department of Cell Biology
The Scripps Research Institute
10550 North Torrey Pines Road
La Jolla, California 92037

Summary

Mus81, a fission yeast protein related to the XPF subunit of ERCC1-XPF nucleotide excision repair endonuclease, is essential for meiosis and important for coping with stalled replication forks. These processes require resolution of X-shaped DNA structures known as Holliday junctions. We report that Mus81 and an associated protein Eme1 are components of an endonuclease that resolves Holliday junctions into linear duplex products. Mus81 and Eme1 are required during meiosis at a late step of meiotic recombination. The *mus81* meiotic defect is rescued by expression of a bacterial Holliday junction resolvase. These findings constitute strong evidence that Mus81 and Eme1 are subunits of a nuclear Holliday junction resolvase.

Introduction

Holliday junctions (HJs) are 4-stranded DNA crossover structures postulated as transient intermediates during genetic recombination and repair (Holliday, 1964; Szostak et al., 1983). Cleavage of the X-shaped HJs across an axis, performed by an HJ resolvase, is required to disentangle homologous duplexes. Recent studies suggest that HJs also arise at stalled replication forks (Seigneur et al., 1998). Thus, uncovering how HJs are resolved is vital for understanding mechanisms of genetic recombination, chromosomal replication, and genome maintenance.

Physical and genetic evidence for HJ formation exists from a number of different experimental systems. X-structures formed during meiosis have been observed in the budding yeast *Saccharomyces cerevisiae* (Collins and Newlon, 1994; Schwacha and Kleckner, 1994). Evidence for replication associated HJs was originally obtained with *E. coli* (Seigneur et al., 1998). These HJs are thought to form by annealing of nascent strands at a stalled replication fork (known as fork regression). Evidence is mounting that HJs are an integral part of replication in eukaryotes. HJs accumulate at the rDNA locus during normal replication in *S. cerevisiae*, and this accumulation is enhanced by mutations in DNA replication polymerases α and δ (Zou and Rothstein, 1997). X-structures were shown to form between sister chromatids during DNA replication in *Physarum* (Benard et al., 2001).

[3] Correspondence: prussell@scripps.edu
[4] These authors contributed equally.

Mutants of the fission yeast *Schizosaccharomyces pombe* that lack Rqh1 DNA helicase display enhanced mitotic recombination and are unable to segregate chromosomes when grown with the replication inhibitor hydroxyurea (Stewart et al., 1997). These phenotypes are partially rescued by expression of RusA, a bacterial HJ resolvase, indicating that Rqh1 is involved in branch migration of HJs that arise at regressed replication forks (Doe et al., 2000).

The best characterized HJ resolvase is RuvC of *E. coli*, which is part of the RuvABC complex that branch migrates and cleaves HJs (Bennett et al., 1993). Interestingly, there are no eukaryotic sequence counterparts of bacterial resolvases, although eukaryotes have mitochondrial HJ resolvases that may be ancestrally related to RuvC (Lilley and White, 2001). Recent studies suggest that HJ branch migration and resolvase activities may associate in calf testes and mammalian cell lines (Constantinou et al., 2001), but eukaryotic nuclear HJ resolvases have thus far eluded identification.

The ERCC1-XPF family of heterodimeric enzymes constitute another interesting class of structure-specific endonucleases. ERCC1-XPF, which has no bacterial orthologs, cuts duplex DNA with a defined polarity on the 5′ side of a junction between double-strand and single-strand DNA (Davies et al., 1995; Sijbers et al., 1996). ERCC1-XPF is essential for nucleotide excision repair (NER), where it incises the damaged strand on the 5′ side of the lesion (Evans et al., 1997; Sijbers et al., 1996). The ERCC1-XPF family of nucleases also appear to participate in various recombination pathways (Paques and Haber, 1999), although Rad1-Rad10 in budding yeast (XPF and ERCC1 homologs, respectively) have no defect in meiotic recombination frequencies and exhibit normal levels of spore viability (Higgins et al., 1983; Snow, 1968). In contrast, *Drosophila melanogaster* MEI-9, an XPF homolog, is required for normal levels of meiotic recombination (Sekelsky et al., 1995).

Mus81, a novel XPF-related protein, was recently discovered through its association with the replication checkpoint kinase Cds1 in fission yeast and the recombination repair protein RAD54 in budding yeast (Boddy et al., 2000; Interthal and Heyer, 2000). Strikingly, fission yeast *mus81* cells exhibit phenotypes expected of an HJ resolvase mutant (Boddy et al., 2000). Mus81 is important for viability in a variety of circumstances that impede replication fork progression, such as unrepaired thymine dimers, nucleotide starvation and compromised DNA polymerase alleles. Mus81 is essential in *rqh1* cells of fission yeast, which are thought to accumulate HJs during DNA replication (Doe et al., 2000). Moreover, Mus81 is required for production of viable spores, a process that is thought to depend on HJ resolution prior to meiosis I (Boddy et al., 2000; Interthal and Heyer, 2000). These findings led us to propose that Mus81 is involved in resolution of HJs (Boddy et al., 2000).

Here we report further characterization of Mus81. We describe Eme1, a novel Mus81 binding protein. Mus81 and Eme1 are essential for meiosis, being required at a late step of meiotic recombination. The *mus81* meiotic

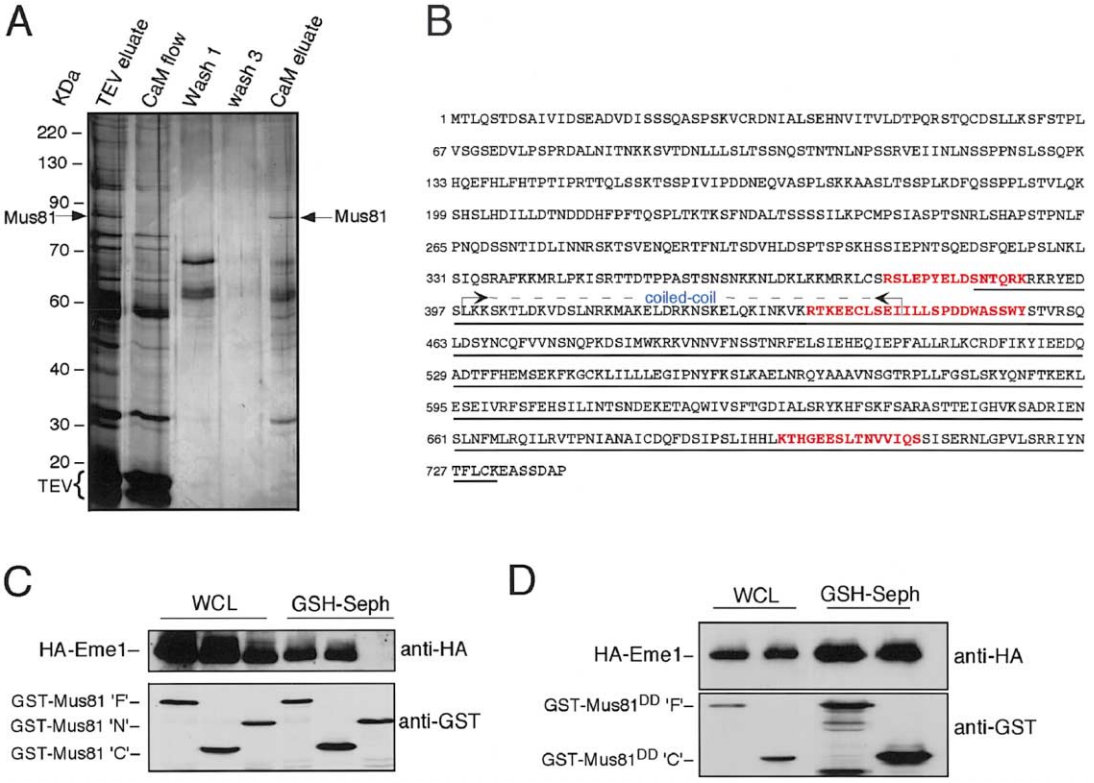

Figure 1. Purification of Mus81-TAP and Identification of Eme1

(A) Silver-stained SDS gel of Mus81-TAP purification. TEV eluate; TEV cleavage products from IgG column. CaM flow; flow through from TEV eluate passed over calmodulin affinity column. Wash 1,2; calmodulin column washes. CaM eluate; eluate from the calmodulin column used for tandem mass spectrometry. The position of Mus81 is indicated and Eme1 is expected to run just below this position. However, we have not established which of these faint bands represents Eme1.

(B) Peptide sequence of Eme1. Eme1 peptides obtained by mass spectrometry are shown in red. The region of Eme1 found to interact with Mus81 in the yeast two-hybrid screen is underlined. Predicted coiled-coil domain is indicated.

(C) Confirmation of in vivo interaction of Mus81 with Eme1. GST-Mus81 fusion proteins; "F", full; "N", N terminus and "C", C terminus were expressed in a strain expressing HA epitope tagged Eme1. HA-Eme1 is detected in GST-Mus81 "F" and "C" but not "N" precipitates isolated with GSH-Sepharose. WCL, whole cell lysate.

(D) Interaction of Eme1 with the Mus81^{DD}. GST-Mus81^{DD} "F" and "C" were expressed in an HA-Eme1 strain. HA-Eme1 coprecipitated with both GST-Mus81^{DD} proteins.

defect is rescued by expression of RusA. Mus81 and Eme1 are components of an endonuclease that resolves HJs in vitro by a mechanism unlike that of previously characterized resolvases. These findings provide strong evidence that Mus81 and Eme1 are components of an HJ resolvase.

Results

Mus81 Associates with Eme1

In the light of the similarity to XPF, we suspected that Mus81 is a subunit of an endonuclease. Therefore, experiments were undertaken to identify Mus81 binding partners. A strain was engineered to express Mus81-TAP from the *mus81*$^{+}$ genomic locus. TAP consists of Protein A and calmodulin binding domains separated by a TEV protease cleavage site (Rigaut et al., 1999). Mus81-TAP strains appeared identical to wild-type (WT), indicating that Mus81-TAP was functional. Mus81 was visible as a silver stained band in the eluate from the IgG column (Figure 1A). Mus81 and associated proteins were eluted from the calmodulin column, trypsinized, and subjected to tandem mass spectrometric (MS/MS) analysis (Figures 1A and 1B). This analysis identified three peptides from a 738 amino acid protein encoded by a gene that we subsequently named *eme1*$^{+}$ (*e*ssential *m*eiotic *e*ndonuclease 1). Eme1 has no sequence homology to ERCC1. We also used the yeast two-hybrid method to screen for proteins that interact with full length Mus81. One of the clones identified by this approach encoded the C-terminal half of Eme1 (Figure 1B).

To further define the interaction of Mus81 and Eme1, GST-Mus81 was produced in cells that expressed epitope tagged Eme1 (3HA-Eme1) from the *eme1*$^{+}$ genomic locus. Full-length and the C terminus of Mus81 bound 3HA-Eme1, whereas the N terminus of Mus81 failed to bind 3HA-Eme1 (Figure 1C). These results indicated that Eme1 and Mus81 interact via their C-terminal regions. Interestingly, Mus81 shares homology with the C terminus of RAD1 and XPF, and these regions are required for formation of RAD1-RAD10 and ERCC1-XPF complexes (Bardwell et al., 1993; de Laat et al., 1998).

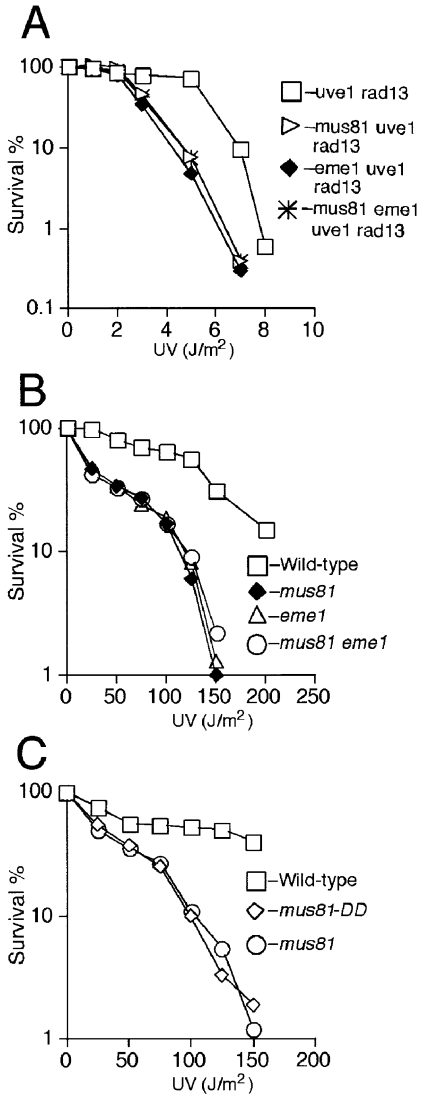

Figure 2. Mus81 and Eme1 Function in the Same Pathways of UV Resistance

(A) Codependent functions of Mus81 and Eme1 for tolerance of irreparable UV lesions. UV sensitivity in a *uve1 rad13* background was enhanced by *mus81* and *eme1* mutations. The quadruple mutant was no more UV sensitive than either triple mutant.

(B) In a repair proficient background (*uve1*$^+$ *rad13*$^+$), *mus81* and *eme1* mutations enhanced UV sensitivity and the *mus81 eme1* double mutant was no more UV sensitive than either single mutant.

(C) The *mus81-DD* mutant was as UV sensitive as the *mus81* delete strain.

Codependent Functions of Mus81 and Eme1 in UV Damage Resistance

Deletion of *mus81*$^+$ enhances the UV sensitivity of *rad13 uve1* cells that are unable to remove thymine dimers, which indicates that Mus81 helps to resolve recombination intermediates that form at stalled replication forks (Boddy et al., 2000). We tested whether Mus81 and Eme1 function in the same pathway of UV damage tolerance. An *eme1 rad13 uve1* strain showed increased UV sensitivity compared to a *rad13 uve1* strain (Figure 2A). The same degree of UV sensitivity was obtained with *mus81 rad13 uve1* cells (Figure 2A). A *mus81 eme1 rad13 uve1* quadruple mutant strain was no more sensitive to UV than either triple mutant (Figure 2A). This relationship between Mus81 and Eme1 was replicated in a *rad13*$^+$ *uve1*$^+$ thymine dimer repair proficient background (Figure 2B). These data showed that Mus81 and Eme1 work in the same pathway of UV damage tolerance.

Mus81 and Eme1 Are Required for a Recombination Step in Meiosis

Spores, the products of meiosis in yeast, are highly inviable in *mus81* mutants (Boddy et al., 2000; Interthal and Heyer, 2000). *eme1* mutants displayed a similar phenotype, yielding ~1% viable spores, as compared to ~80% in wild-type (Figure 3A). These findings further underscored the similar phenotypes of *eme1* and *mus81* mutants.

We investigated if poor spore viability in *mus81* and *eme1* mutants was caused by a recombination defect. Rec6 and Rec12 are required for formation of double-strand breaks (DSBs) that initiate meiotic recombination (Lin and Smith, 1994). *rec6* or *rec12* mutants yield ~20% viable spores, presumably due to residual homolog pairing in the absence of recombination (Lin and Smith, 1994). Epistasis studies were performed with *mus81* and *eme1* mutations in *rec6* or *rec12* backgrounds. Interestingly, *mus81 rec6* and *eme1 rec6* double mutants yielded ~20% viable spores, an amount equivalent to *rec6* mutants (Figure 3A). Very similar results were obtained in the epistasis studies with *rec12* (Figure 3A). These results showed that Mus81 and Eme1 are required after initiation of recombination.

We investigated whether NER enzymes have a meiotic function in fission yeast. Spore viability was measured using *rad16* and *swi10* homozygous diploids, defective for the XPF and ERCC1 homologs, respectively (Carr et al., 1994; Rodel et al., 1997). These mutants exhibited no defect in spore viability (Figure 3A). These findings demonstrated that the Rad16-Swi10 endonuclease is not required for meiosis and highlighted the functional distinctions between Mus81 and Rad16.

Wild-type meiosis I and II nuclear divisions produce asci containing four haploid spores (Figure 3B). Interestingly, *mus81* asci contained erratic numbers of spores (1–4) that were variable in size (Figure 3B). Spore size usually reflects ploidy; that is, diploid spores are larger than haploids. The majority of *mus81* asci contained one large spore with two or three much smaller spores. Invariably, the largest spore contained all or most of the DNA (Figures 3B and 3C). These data indicated that *mus81* mutants failed to correctly segregate chromosomes during meiosis I.

Rhp51, a Rad51/RecA homolog in fission yeast (Muris et al., 1993), is presumed to be required for the strand invasion step in genetic recombination. DSBs accumulate in *rhp51* mutants (Zenvirth and Simchen, 2000), which accounts for the poor spore viability of *rhp51* mutants (Boddy et al., 2000). However, *rhp51* mutants show mainly four DAPI stained foci per ascus, similar to wild-type (Figures 3B and 3C). These data suggest that *rhp51* mutants regularly complete meiosis I and II. Thus, unlike *rhp51*, the *mus81* meiotic defect cannot be explained by DSB persistence. Unresolved recombina-

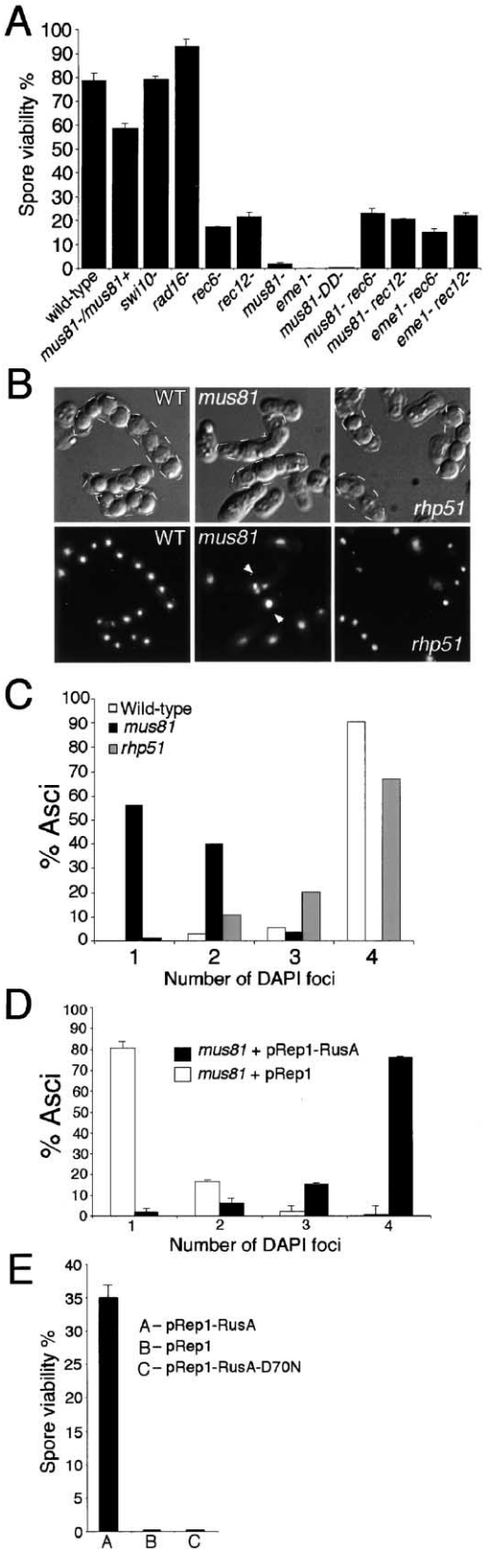

Figure 3. Meiotic Defects of *mus81* and *eme1* Mutants

(A) Spores from *mus81* and *eme1* asci exhibit very poor viability. This defect is rescued by *rec6* and *rec12* mutations that prevent meiotic recombination. All diploids were homozygous with the exception of the *mus81*$^{-}$/*mus81*$^{+}$ heterozygote.

(B) DNA segregation defects in *mus81* asci. WT, *mus81* and *rhp51* asci were visualized by DIC microscopy to show spores (upper panels) and stained with DAPI to visualize DNA (lower panels). Mature asci in each DIC panel are outlined with a dashed line. Arrowheads indicate aberrant meiotic products in *mus81* asci.

(C) The majority of *mus81* asci contain a single focus of DNA. The number of discreet DAPI stained foci per ascus was ascertained. Approximately 100 mature asci were counted for each strain.

(D) The segregation defect observed in *mus81* meioses is corrected by expression of RusA. *mus81* mutants expressing RusA were mated and mature asci were examined microscopically. The number of discreet DAPI stained foci per ascus was ascertained.

(E) The low spore viability resulting from *mus81* meioses is substantially rescued by RusA. *mus81* mutants carrying pRep1, pRep1-RusA, or catalytically dead pRep1-RusA-D70N were mated and the resultant spore viabilities determined. Data shown are representative of four independent experiments.

tion intermediates, such as HJs, are consistent with the segregation defects observed in *mus81* mutants.

RusA, a Bacterial HJ Resolvase, Suppresses *mus81* Meiotic Defect

From the genetic and cytological data on *mus81* mutant meioses, we concluded that Mus81 is required for HJ resolution. This hypothesis was tested by expressing a highly specific bacterial HJ resolvase, RusA, in *mus81* mutants (Doe et al., 2000). The SV40 nuclear localization signal (NLS) was added to the N terminus of RusA to ensure its nuclear localization (Doe et al., 2000). The cytological defects of *mus81* mutant meioses were largely corrected by the overexpression of RusA (Figure 3D). Approximately 75% of these asci contained four spores of apparently equal DNA content. Strikingly, zygotic meioses using *mus81* mutants that expressed RusA yielded a spore viability of about 35% (Figure 3E). This value was approximately 350-fold greater than the vector control (Figure 3E). Importantly, the meiotic rescue of *mus81* mutants was dependent on the endonuclease activity of RusA. RusA-D70N, which lacks endonuclease activity but still binds HJs (Doe et al., 2000), was unable to rescue the *mus81* mutant meiotic defect (Figure 3E). Both wild-type RusA and the D70N mutant were equally expressed (data not shown). These data strongly support our conclusion that Mus81 and Eme1 are required for resolving HJs that form between homologous chromosomes during meiosis.

Predicted Endonuclease Active Site Is Essential for Mus81 Function

Having established that Mus81 is required for HJ resolution during meiosis, we sought evidence that Mus81 and Eme1 are components of an HJ endonuclease. We first investigated the domain of Mus81 that is predicted to form the endonuclease active site. The C terminus of Mus81 contains a predicted endonuclease active site, VERKXXDD, conserved in XPF, in which an aspartic acid residue is proposed to coordinate the divalent cation required for catalysis (Aravind et al., 1999). A *mus81* genomic replacement was constructed in which the aspartic acid codons at 359–360 in the VERKXXDD sequence were mutated to alanine to form the allele

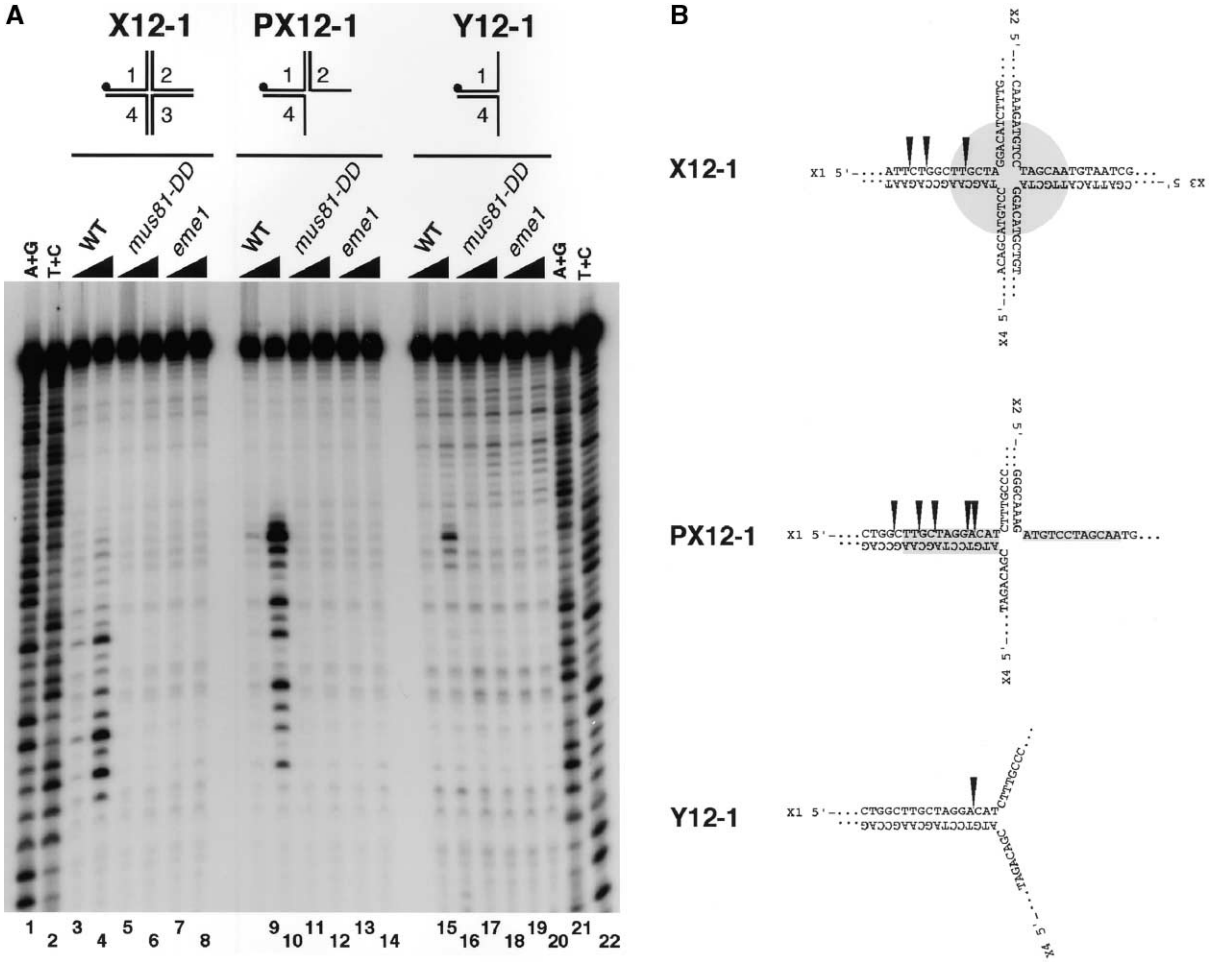

Figure 4. Mus81 and Eme1 Are Components of a Structure-Specific Endonuclease

(A) Schematic representations of the structure of each DNA substrate are shown above the gel. Each structure contains a 5′ labeled oligonucleotide X1 as indicated by the black dot. The DNA substrates were incubated with 0.5 μl and 6 μl of TEV-eluates obtained from the Mus81:TAP strain (lanes 3, 4, 9, 10, 15, 16), the *mus81-DD:TAP* mutant strain (lanes 5, 6, 11, 12, 17, 18), or the *mus81:TAP eme1* mutant strain (lanes 7, 8, 13, 14, 19, 20). Reactions were analyzed on a 12% sequencing gel. Maxam-Gilbert G+A and T+C sequencing ladders derived from oligonucleotide X1 were run in parallel (lanes 1, 2, 21, 22).

(B) The main sites of cleavage as determined from the Maxam-Gilbert sequencing ladders, are indicated by arrows on each DNA structure. The area shaded in gray represents the 12 bp homology region that allows the junction to migrate in X12 and PX12.

mus81-DD. Mus81^{DD} abundance was similar to wild-type Mus81 (data not shown) and Mus81^{DD} interacted normally with Eme1 (Figure 1D). The *mus81-DD* mutant appeared identical to the *mus81* deletion mutant in UV sensitivity and spore viability assays (Figures 2C and 3A). These data showed that Mus81 function requires at least one aspartic acid residue at 359–360. The *mus81-DD* allele was a valuable tool in the characterization of Mus81-associated endonuclease activity, as described below.

Structure-Specific DNA Endonuclease Activity Associated with Mus81-Eme1

The genetic properties of *mus81* and *eme1* mutants provided compelling evidence that Mus81-Eme1 was required for resolution of HJs in vivo, we therefore asked if Mus81 has an associated endonuclease activity. In vitro nuclease assays were set up with various DNA substrates (Figure 4A). They are all derived from the same set of four oligonucleotides. X12 was made by annealing all four oligonucleotides. It has a 12 base pair region of homology in its center allowing the junction to migrate (Parsons et al., 1990). Y12, made with oligonucleotides X1 and X4, is a typical ERCC1-XPF substrate. The double-strand/single-strand junction of Y12 is fixed. The partial X-substrate PX12 was made with oligonucleotides X1, X2, and X4. The junction can slide in PX12.

Substrates prepared with oligonucleotide X1 radiolabeled at its 5′ terminus were incubated with TEV-eluate from the Mus81-TAP strain and analyzed on a denaturing sequencing gel (Figure 4A). Defined cleavage products were detected with each substrate (Figure 4A). The nuclease activity was ATP independent and the cleavage patterns were unchanged in the presence of ATP (data not shown). No nuclease activity was detected in the absence of Mg^{2+}, and optimum cutting was found at 2.5 mM Mg^{2+} in titration experiments using up to 20 mM Mg^{2+} (data not shown).

Three major cleavage products were obtained with X12 (Figure 4A, lane 4). One product resulted from a cut within the homology region, whereas the others resulted from cuts three and five nucleotides 5′ to this region (Figure 4B). No sites were found 3′ to the homology region, suggesting that the enzyme cuts only on the 5′ side of the junction. Cutting of Y12 was weak relative to X12 (Figure 4A). The major cleavage site on Y12 was mapped in the duplex arm, 3 nucleotides to the 5′ side of the fixed junction (Figure 4B). No cleavage was detected when Y12 was labeled at the 3′ end of oligonucleotide X4 (data not shown). This result indicates that Mus81 cuts DNA in a similar manner to ERCC1-XPF, introducing cuts on one strand of the duplex 5′ to the double-strand/single-strand junction. PX12 was an excellent substrate of Mus81 (Figure 4A). Four cleavage sites were mapped within the homology region of PX12. A fifth site was found in the heterology region, 1 nucleotide to the 5′ side of the homology core. As for X12, no cut sites were found 3′ to the homology core of PX12 (Figure 4B).

To verify that intact Mus81 and Eme1 were required for nuclease activity, we carried out reactions with TEV-eluates from *mus81-DD:TAP* and *mus81-TAP eme1* strains. TEV-eluates from these strains yielded Mus81-TAP in amounts similar to wild-type (data not shown) but they had no nuclease activity (Figure 4A). These results showed that the nuclease activity requires Eme1 and an intact VERK domain in Mus81.

X-Structure Resolved into Linear Duplex Products

The generation of nicks of like polarity in opposing strands is the essential feature of HJ resolution. Resolution of HJs in vitro can be visualized by conversion of an X-structure into linear double-strand products detected by native gel electrophoresis. Mus81-Eme1 dependent nuclease was tested in this assay (Figure 5). ATP was added to some reactions to determine if a branch migration activity copurified with Mus81. This activity would produce Y structures by driving branch migration through the heterologous ends of opposing arms of the junction. Two migration controls, a Y structure and a linear duplex made by annealing oligonucleotide X1 with its complementary sequence, were run in parallel.

The TEV-eluate from Mus81-TAP cells converted a fraction of X12 into linear duplex products (Figure 5A), consistent with the coordinated generation of symmetric or closely symmetric cuts on opposed strands (Figure 5B). No Y structures were formed in the presence of ATP, indicating absence of branch migration activity in the TEV-eluate (Figure 5A). Cleavage of PX12 generated a product that migrated faster than the linear duplex product obtained with X12 (Figure 5A). This result is consistent with cleavage of oligonucleotide X1 to generate double-strand/single-strand hybrids (Figure 5C). No cleavage products were observed with TEV-eluates obtained from the *mus81-DD* and *eme1* mutant strains (data not shown). These data show that Mus81-Eme1 complex resolves HJs into linear duplex products.

Cleavage Sites Mapped on Each Arm of X-Structure Substrates

To map the cleavage sites on each arm of the junction, we made four preparations of X12, each labeled on a

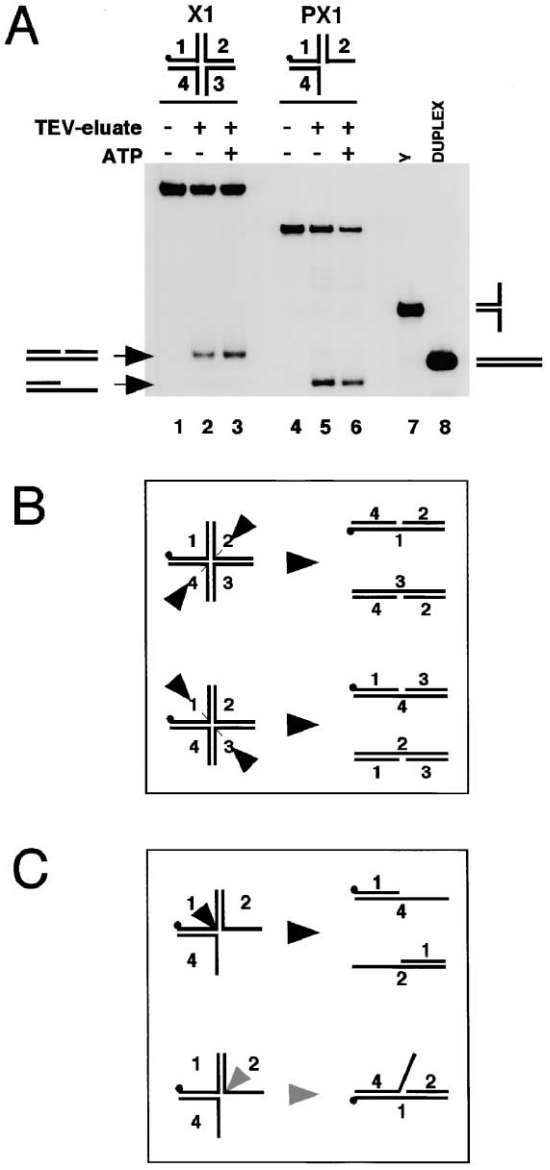

Figure 5. Resolution of the X-Structure into Linear Duplex Products

(A) The X12 and PX12 structures were incubated with 3 μl of either TEV-elution buffer (lanes 1, 4) or TEV-eluate obtained from the Mus81:TAP strain (lanes 2, 3, 5, 6). Reactions were carried out in the absence or the presence of ATP as indicated. Reaction products were analyzed on a native PAGE gel. Markers run in parallel indicate the migration of a Y structure (lane 7) and a linear duplex made by annealing oligonucleotide X1 to an oligonucleotide of complementary sequence (lane 8).

(B) Schematic representation of products generated by cleavage of an X-structure on oligonucleotides 2 and 4 or 1 and 3.

(C) Schematic representation of products generated by cleavage of the partial X-substrate. Cutting on oligonucleotide X1 (black arrowhead) generates double-strand/single-strand hybrids that migrate faster than a linear duplex made of full-length complementary oligonucleotides (A, lanes 5 and 6). Cutting on oligonucleotide X2 (gray arrowhead) generates a duplex product that bears a 5′ single-strand flap corresponding to part of oligonucleotide X4 and which should migrate slower than a linear duplex. No such product was detected, indicating that the partial X-substrate was preferentially cut on oligonucleotide X1 between the two juxtaposed duplex arms.

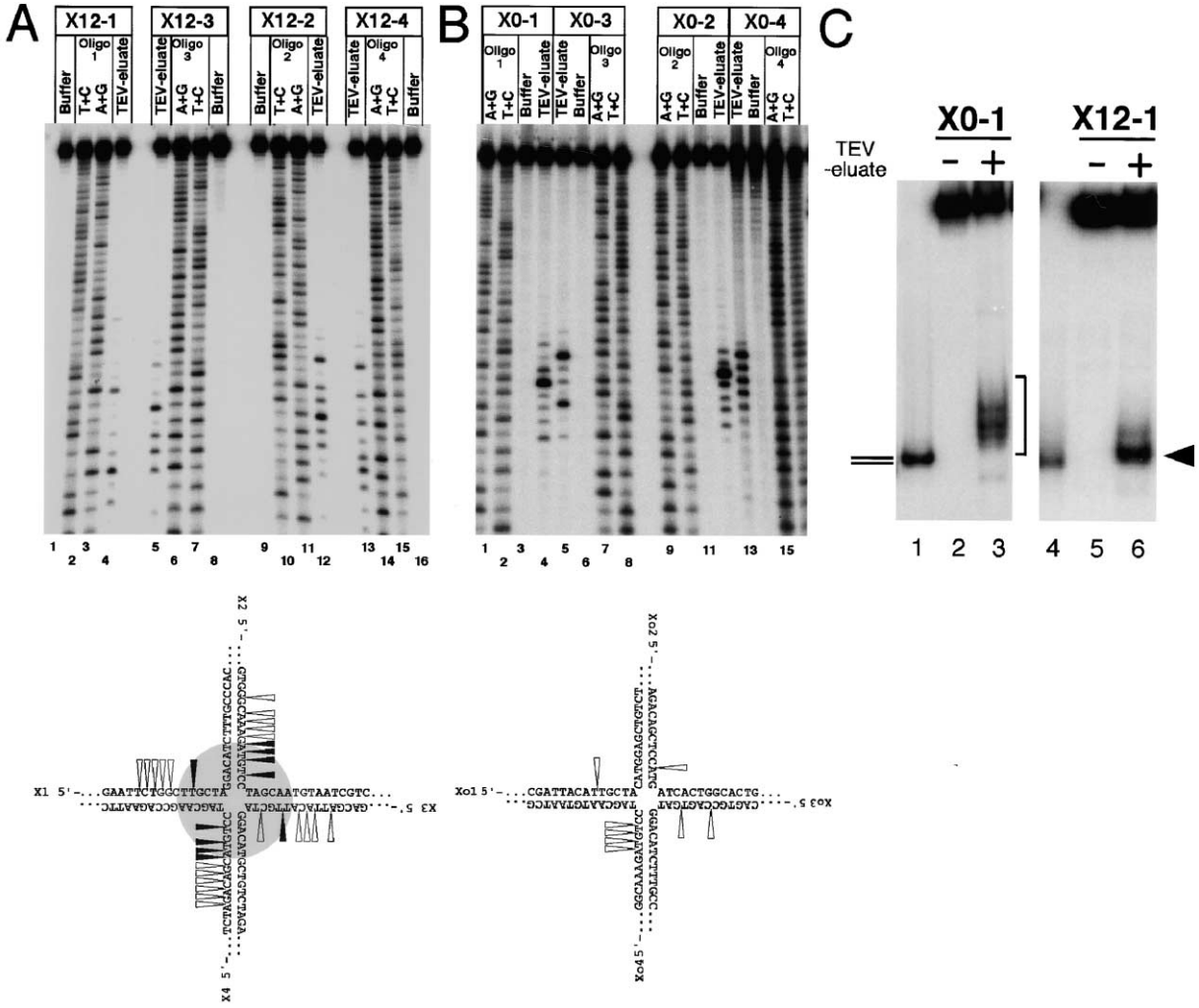

Figure 6. Mapping of Cleavage Sites on Each Arm of Migratable and Fixed Junctions

(A) Four different X12 structures, each labeled on a different oligonucleotide, were incubated with 3 μl of either TEV-elution buffer (lanes 1, 8, 9, 16) or TEV-eluate obtained from the Mus81:TAP strain (lanes 4, 5, 12, 13). Reactions were analyzed on a 12% sequencing gel along with Maxam-Gilbert sequencing ladders (lanes 2, 3, 6, 7, 10, 11, 14, 15). Note that 5 min reactions were used for mapping the cleavage sites because cuts in the heterology regions accumulated during longer incubations (data not shown). Cleavage sites are indicated on each arm of the X-structure. Closely symmetric sites on opposing strands across the junction that were found inside the region of homology are indicated by the black arrows. Nonsymmetric sites in the region of homology or sites mapped in the heterologous sequences are indicated by open arrows.

(B) Cleavage sites generated on a fixed junction were mapped on four different X0-structures, each labeled on a different oligonucleotide. The main cleavage sites are indicated on each arm of the structure.

(C) Cleavage products generated with X0 (lanes 2 and 3) and X12 (lanes 5 and 6) were analyzed on a native PAGE gel. A linear duplex control was run in lanes 1 and 4. The bracket alongside lane 3 indicates the diffuse migration of the linear duplex products generated with X0. The arrowhead alongside lane 6 indicates the position of the linear duplex products generated with X12.

different oligonucleotide. With oligonucleotides X2 and X4, clusters of potentially symmetric cuts were detected in the homology domain (Figure 6A). The major cleavage site in the homology domain of oligonucleotide X1 was offset by one nucleotide from the major cleavage site on oligonucleotide X3. Cleavage sites were also found in the regions of heterology on all four arms. Strikingly, these sites were all located within six nucleotides 5′ to the homology core. The proportion of cleavage sites in the heterology region appeared to increase upon longer incubations (data not shown). No cuts on any of the four oligonucleotides were found 3′ to the region of homology, consistent with the polarity of the enzyme (Figure 4). Despite the resolution of X12 into linear duplex products (Figure 5), and the presence of a number of apparently symmetric cuts, we were unable to demonstrate ligation of the linear duplex products (data not shown). This result might be explained if these products have small gaps or flaps resulting from slightly offset cuts. Such products generated by an HJ resolvase in vivo could be processed by flap endonucleases and gap fill-in reactions prior to ligation.

We also assayed the ability of Mus81-Eme1 complex to cleave a fixed X-structure (X0) that lacked a central

homology domain (Figure 6B). Major cut sites were mapped 2 to 7 nucleotides 5′ to the junction in all fours arms. The major cut sites appeared to be offset by 1 to 3 nucleotides across the junction. The linear duplex products generated from X0 migrated slowly as a diffuse group of bands as compared to X12 products (Figure 6C). It appears that the presence of a homology core contributes to coordinated cleavage across the junction. These results suggest that Mus81-Eme1 cleaves HJs in a fundamentally different manner compared to prokaryotic HJ resolvases, as discussed below.

Discussion

We have reported that *mus81* and *eme1* mutants have meiotic and replication defects that are exactly those expected of an HJ resolvase mutant. Strikingly, *mus81* meiotic defects are rescued by a bacterial HJ resolvase. Mus81 and Eme1 are components of a nuclease that cleaves HJs in vitro to yield linear duplexes. This enzyme exhibits a preference for DNA structures having juxtaposed duplex arms, such as those found at HJs and stalled replication forks. Overall, these genetic and biochemical data provide compelling evidence that Mus81 and Eme1 are components of a nuclear HJ resolvase in fission yeast.

Meiotic Role of Mus81

A mutant defective in the processing of HJs should be unable to complete meiosis due to a chromosome segregation defect arising from unresolved recombination intermediates. Here we have demonstrated that the poor viability of *mus81* spores is closely connected to recombination. We found that preventing DSB formation with *rec6* or *rec12* mutations obviated the need for Mus81. Therefore, *rec6* and *rec12* mutations are epistatic to *mus81*. These findings show that Mus81 is required to resolve recombination intermediates during meiosis.

The striking cytological differences between *mus81* and *rhp51* asci provide additional insight into Mus81 function. Rhp51 is required for strand invasion of the intact homologous duplex following DSB formation (Paques and Haber, 1999). Despite persistent DSBs, *rhp51* mutants proceed with meiotic nuclear division to produce four spores of roughly similar DNA content. These findings indicate that *S. pombe* has no meiotic recombination checkpoint, consistent with other studies (Nabeshima et al., 2001). In contrast to *rhp51* asci, *mus81* asci have variable numbers of spores and most of the DNA is found in the largest spore. This phenotype suggests a defect in which homologous chromosomes are entangled by unresolved crossover events.

The unusual phenotype of *mus81* asci is most consonant with a defect in HJ cleavage. This idea is strongly supported by the remarkably effective rescue of *mus81* meiotic defects by expression of RusA, a highly specific bacterial HJ resolvase. We conclude that the *mus81* meiotic defects are caused by an inability to resolve HJs.

Role of Mus81 in Vegetative Cells

HJs are proposed to arise as a result of replication fork regression (Seigneur et al., 1998); thus, the other phenotype expected of an HJ resolvase mutant is sensitivity to situations that arrest replication. We showed previously that Mus81 is important for tolerance of replication arrest caused by thymine dimers, nucleotide starvation and compromised DNA polymerase alleles (Boddy et al., 2000). The potential for HJ formation is a common theme in all these situations. Strikingly, *mus81* mutations impaired survival of mutants for DNA polymerase δ and α but not ϵ. These findings correlate with studies showing that temperature-sensitive alleles of DNA polymerases α and δ but not ϵ result in X-structure accumulation in *S. cerevisiae* (Zou and Rothstein, 1997).

Regressed replication forks have been proposed to be corrected either by reversal of replication fork regression or by a recombinogenic process that involves HJ resolution (Doe et al., 2000). Rqh1 has properties expected of a helicase that unwinds regressed replication forks (Doe et al., 2000; Stewart et al., 1997), and the human homologs of Rqh1 were shown to unwind HJs in vitro (Constantinou et al., 2000; Karow et al., 2000). It is intriguing that Mus81 is essential for viability in *rqh1* cells (Boddy et al., 2000). Given these facts, it is reasonable to suggest that Mus81 is required for HJ resolution in a recombinogenic pathway that normally operates in parallel with a nonrecombinogenic pathway mediated by Rqh1 at regressed replication forks (Figure 7A).

Mus81-Eme1 Complex

Eme1 and Mus81 are binding partners that define the same genetic epistasis group and enzymatic activity. This situation is highly reminiscent of the Mus81 related protein XPF and its partner ERCC1, although Eme1 and ERCC1 have no significant sequence similarity. Phenotypes associated with loss of Mus81-Eme1 bear little resemblance to those caused by Swi10-Rad16 (ERCC1-XPF homolog) inactivation. Swi10-Rad16 are required for NER, whereas Mus81-Eme1 functions in resolution of HJs. Thus, Mus81 and XPF share a common ancestor, but they have very different cellular functions and associate with apparently unrelated binding partners.

In budding yeast, mutations of *mus81* (also called *slx3*) and a gene known as *mms4* were recently found to cause lethality in an *sgs1* mutant background (Mullen et al., 2001). Sgs1 is the budding yeast homolog of Rqh1. Interestingly, *mus81* and *mms4* were placed in the same genetic epistasis group and their protein products were found to coprecipitate. Mms4 and Eme1 have weak sequence similarity and are probably functionally related. In addition, Eme1 has a weak but statistically significant sequence homolog in *Neurospora crassa* (accession #AL356173). The extreme sequence divergence of Eme1 homologs in fungi may explain why related genes have not been detected in the sequenced genomes of more complex eukaryotes. It is a formal possibility that Eme1 is a fungi-specific protein, but we expect that multicellular organisms have Eme1 functional homologs because Mus81 has clear sequence homologs in a broad range of eukaryotes, including humans (Boddy et al., 2000). In fact, we have recently demonstrated that Mus81 HJ resolvase activity is conserved in humans (Chen et al., 2001 [November issue of *Molecular Cell*]).

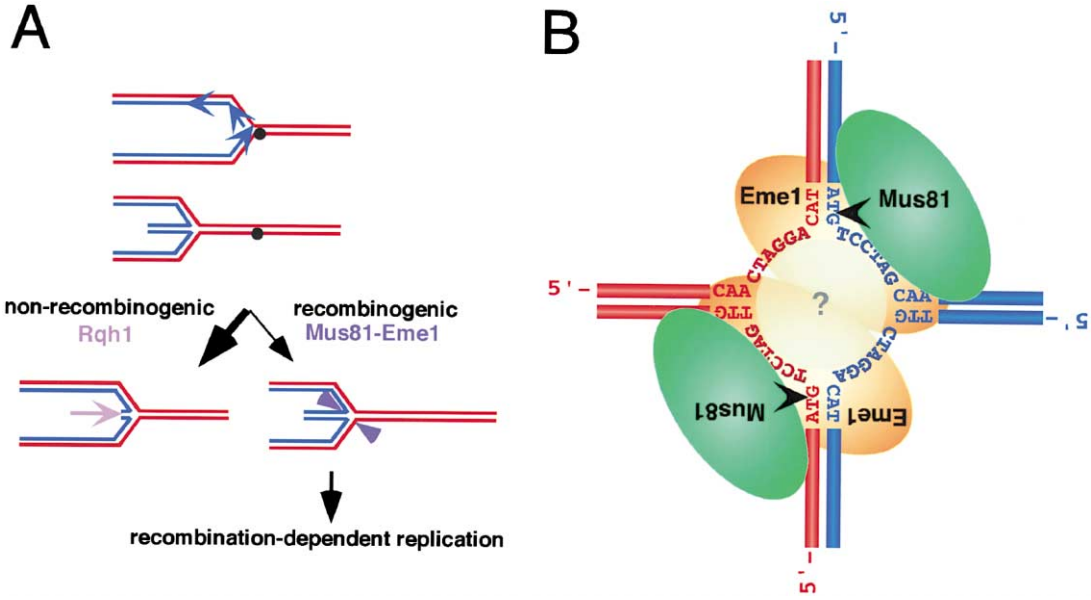

Figure 7. Models for Roles of Mus81-Eme1

(A) An HJ formed at a collapsed replication fork is either reversed by Rqh1 type helicases in a nonrecombinogenic pathway or resolved by a Mus81-Eme1 dependent endonuclease in a recombinogenic pathway.

(B) A "bubble" structure with symmetric double-strand/single-strand DNA junctions and juxtaposed duplex arms could constitute a favored substrate for Mus81-Eme1 dependent endonuclease. Cofactors might help to stabilize the open structure in vivo. Symmetric or closely symmetric cuts on opposing strands would be generated at the double-strand/single-strand DNA junctions and result in HJ resolution.

Resolution of Holliday Junctions by Mus81-Eme1 Dependent Endonuclease

The defining enzymatic feature of an HJ resolvase is the ability to introduce nicks into strands of like polarity across a 4-way helical branch point. The products of this reaction are two linear duplex DNA molecules (Figure 5B). Affinity-purified preparations of Mus81 possess this activity (Figure 5A). This activity requires at least one conserved aspartic acid residue in the conserved VERK domain shared between XPF and Mus81 homologs. This activity also requires Eme1. Thus, Mus81 and Eme1 are essential components of an endonuclease that is required for HJ resolution in vivo and which resolves X-structures into linear duplexes in vitro. Our data leaves uncertain whether Mus81 and Eme1 are the only essential components of this endonuclease, but the analogy to ERCC1-XPF suggests this is a very likely possibility. No other candidate subunits were identified by mass spectrometry, indicating that Mus81 and Eme1 are the core subunits of the resolvase.

Noneukaryotic and mitochondrial HJ resolvases have no sequence homologs in sequenced eukaryotic genomes, and close examination shows that they share no sequence similarity to Mus81 or Eme1. However, Mus81 is related to XPF, thus we expected that Mus81-Eme1 would share some functional properties with ERCC1-XPF endonuclease. Indeed, Mus81-Eme1 cleaved a Y DNA structure on one strand of the duplex 5′ to the junction, indicating a similar polarity to ERCC1-XPF. Importantly, nuclease activity was substantially more pronounced on X-structures. All cleavage sites mapped on the four arms of X12 were within the homology core or a few nucleotides 5′ to that region, but never in the region of heterology 3′ to the homology core. This finding suggests that Mus81-Eme1 cuts X and Y structures in a similar manner, by introducing incisions on duplex DNA 5′ to a double-strand/single-strand junction (Figure 7B). This mechanism is completely unlike that of prokaryotic and mitochondrial resolvases, which have no requirement for a double-strand/single-strand junction (Lilley and White, 2001).

It is noteworthy that the central homology domain of X12 is sensitive to potassium permanganate, which reacts with unpaired thymine residues (West, 1995). Thymine residues outside the homology domain are not sensitive to permanganate, nor are thymines in an X-structure that lacks a homology core in the center. These findings indicate that base pairing around the junction point can be destabilized during branch migration (West, 1995). In vivo, HJs are made entirely of homologous sequences that branch migrate, and one could imagine that additional cofactors might also contribute in vivo to stabilize an open structure. Interestingly, we found that Mus81-Eme1 complex could also cut fixed X-structures. These findings indicate that Mus81-Eme1 complex might itself contribute to the opening of the X-substrate in its center (Figure 7B). However, the major cuts generated on fixed X-structures were not paired symmetrically across the junction. The efficiency of the opening of the double helix is influenced by the sequence context. Therefore, the extent of opening of an X-structure that can migrate in its center is expected to be symmetric on opposed arms but not on a fixed X-structure that has different sequences on all four arms. Hence, double-strand/single-strand junctions that arise from the opening of a migratable junction would be symmetrically opposed. If the cleavage by Mus81-Eme1 is orientated by the position of such junc-

tions, then symmetric cuts should be generated on a migratable junction but not on a fixed junction. A bubble structure with stabilized double-strand/single-strand junctions and juxtaposed double-strand arms could constitute a favored substrate for Mus81-Eme1 dependent cutting (Figure 7B).

Cleavage of Partial X

The partial X-structure PX12 was an excellent substrate for Mus81-Eme1, particularly when compared to Y12. These findings suggest that Mus81-Eme1 requires two juxtaposed double-strand arms for efficient DNA binding and positioning of the DNA in its catalytic site. Mus81-Eme1 converted the PX12 into a small cleavage product that migrated in a native gel faster than linear duplex product generated from X12 (Figure 5A). This finding is consistent with oligonucleotide X1 being cleaved near the junction, releasing a cleavage product made of full-length oligonucleotide X4 and part of cleaved oligonucleotide X1 (Figure 5C). If Mus81-Eme1 has a strong proclivity to cleave Y structures, PX12 should also be cleaved on oligonucleotide X2 near the junction (Figure 5C). This cleavage would produce duplex DNA with a single-strand flap that would migrate slower in a native gel relative to a linear duplex (Figures 5A and 5C). No such product was detected, indicating a strong preference for cleavage of the partial X-structure on oligonucleotide X1 between the two juxtaposed duplex arms. This prediction was confirmed by comparing the efficiency of cleavage of partial X-substrates labeled on oligonucleotides X1 or X2 (data not shown). These observations support the hypothesis that Mus81-Eme1 requires two juxtaposed double-strand DNA arms to optimally bind and cleave its substrate. This substrate preference is completely unlike that of ERCC1-XPF family members.

PX12 cleavage by Mus81-Eme1 is interesting in light of the proposal that HJ resolvases act in a two-step manner (Lilley and White, 2001). In this model, the first cut of an HJ is relatively slow and rate-limiting. This cut would then increase the flexibility of the DNA structure, helping it to adopt an optimum position relative to the catalytic site for the second cut to occur on the opposing strand (Lilley and White, 2001). The increased flexibility between the two double-strand arms of the partial X-structure might help the enzyme to ideally position the substrate in its catalytic site.

The partial X-structure could constitute a simplified model of a stalled replication fork, in which synthesis on one of the strands has stalled while synthesis on the other strand has continued. A role of Mus81-Eme1 in resolving these structures would be consistent with the high sensitivity of *mus81* mutants to a variety of situations that block replication, although there is no experimental evidence for processing of stalled forks that have not regressed. Indeed, the sensitivity of *mus81* mutants to situations that stall replication might be entirely explained by the ability of Mus81-Eme1 complex to resolve HJs, which have been demonstrated to occur at stalled replication forks (Seigneur et al., 1998).

Conclusions

We have presented genetic and physiological evidence that Mus81 and Eme1 are essential components of a nuclear Holliday junction resolvase. The phenotypes caused by *mus81* and *eme1* mutations are precisely those expected of a resolvase mutant, a fact underscored by the rescue of the *mus81* meiotic defect by RusA. Mus81-Eme1 introduces paired incisions on opposing strands of an X-structure, but it does so in a manner completely unlike that of previously characterized resolvases. It will be fascinating to determine exactly how Mus81-Eme1 interacts with X-shaped DNA, as this holds the key to understanding how it resolves Holliday junctions.

Experimental Procedures

General Techniques

Fission yeast methods and media have been described (Moreno et al., 1991). UV sensitivity studies were performed as described (Boddy et al., 2000) and data shown are representative of two or more experiments. Spore viability assays were performed by mixing cells of opposite mating types and incubating on supplemented SSA media for 3 days to obtain mature asci. Asci were treated with glusulase to obtain free spores. Spores were counted with a hemacytometer and plated on YES media.

Strains and Plasmids

Strains used in this study are *ura4-D18* and *leu1-32* unless otherwise stated: PR109, wild-type; NB2554, *mus81::kanMx6*; PS2345, *rhp51::ura4*$^+$; PS2403, *uve1::LEU2 rad13::ura4*$^+$; NB2558, *mus81::kanMx6 uve1::LEU2 rad13::ura4*$^+$; NB2823, *mus81-TAP:kanMx6*; NB2824, *eme1::kanMx6*; NB2825, *nmt1-3HA-eme1:kanMx6*; NB2826, *mus81::kanMx6 eme1::kanMx6*; NB2827, *mus81*^{D359,360A}*-TAP:kanMx6* (referred to as *mus81-DD*); NB2828, *eme1::kanMx6 uve1::LEU2 rad13::ura4*$^+$; NB2829, *mus81::kanMx6 eme1::kanMx6 uve1::LEU2 rad13::ura4*$^+$; NB2830, *mus81::kanMx6 rec6::LEU2*; NB2831, *mus81::kanMx6 rec12::LEU2*; NB2832, *eme1::kanMx6 rec6::LEU2*; NB2833, *eme1::kanMx6 rec12::LEU2*; PS2443, *swi10::ura4*$^+$; PS2445, *rad16::ura4*$^+$; NB2775, *rec6::LEU2*; NB2776, *rec12::LEU2*. The Bahler PCR method was used to generate strains NB2823-2825 and NB2827 (Bahler et al., 1998); pREPKZ (Shiozaki and Russell, 1997), to express in frame GST fusion proteins. Modified pREP1 was used to express NLS-RusA. The RusA-D70N mutation was made by PCR stitching.

Identification of Eme1

Cells (40 g wet weight) expressing Mus81-TAP at the genomic locus were lysed using a bead beater (Waring) in buffer A (50 mM Tris pH 8, 150 mM NaCl, 2 mM EDTA, 10% glycerol, 0.2% Nonidet P-40, 5 μg/ml each of leupeptin, pepstatin, and aprotinin, and 1 mM PMSF). Mus81-TAP was purified from clarified lysate as described (Rigaut et al., 1999). The final eluate was precipitated with TCA (25% v/v) for 1 hr on ice. The precipitate was pelleted in a bench top microfuge (Eppendorf) at a relative centrifugal force (r.c.f.) of 16. The pellet was washed twice with acetone (−20°C) and air dried. The sample was reduced and alkylated using dithothreitol and iodoacetamide and then sequentially digested with endonuclease lyse-C (Roche) and trypsin (Perceptive Biosystems) (McCormack et al., 1997). The resulting peptide mixture was analyzed by multidimensional protein identification technology (MudPIT) (Link et al., 1999; Washburn et al., 2001) with modifications described by McDonald et al. (submitted). Tandem mass spectra were searched against version 11 of the pompep database to which common contaminants such as keratin and trypsin were added (These sequence data were produced by the *S. pombe* Sequencing Group at the Sanger Centre and can be obtained from ftp://ftp.sanger.ac.uk/pub/yeast/Pombe/Protein_data/New_pompep_V11_30APR2001/pompep_minus_tf). Search results were filtered and grouped using the DTASelect program (Tabb et al., submitted) and identifications confirmed through manual evaluation of spectra. For the yeast two-hybrid screen, full-length Mus81 cDNA was cloned into pAS404 (Nakashima et al., 1999). PAS404-Mus81 was integrated at *TRP1* in *S. cerevisiae* strain Y190 (Harper et al., 1993). This strain was used to screen Mus81 against an *S. pombe* cDNA library (Clontech).

Immunoblotting and Microscopy Techniques

For immunoblotting, cells were lysed using a bead beater in buffer A and resolved in 10% sodium dodecyl sulfate polyacrylamide gels (SDS-PAGE). Proteins were transferred to Immobilon membrane, blocked in 5% milk in TBS and 0.3% Tween-20, and probed with antibodies to the HA epitope. For GST pull down experiments, GST-Mus81 expression was induced from the *nmt1* promoter for 18 hr (Maundrell, 1993). Cells were lysed in buffer A and GSH-Sepharose (Pharmacia) was added to the lysates followed by incubation at 4°C for 1.5 hr with rotation. Complexes were collected by centrifugation and washed three times with buffer A before resuspension in SDS-PAGE loading buffer.

For meiosis studies, cells of opposite mating type were mixed and grown for 3 days on SSA minimal media (Egel and Egel-Mitani, 1974) supplemented with appropriate amino acids but lacking nitrogen. Zygotic asci were fixed in methanol (−80°C) for 10 min. The fixed asci were treated with Zymolyase 100T (0.1 mg/ml) for 10 min at 37°C. Asci were collected by centrifugation and resuspended in 0.1% Triton X-100 for 2 min at room temperature. Asci were then washed three times with phosphate buffered saline (PBSA) and resuspended in a drop of PBSA containing 0.5 μg/ml the DNA stain DAPI. Asci were photographed using a Nikon Eclipse E800 microscope equipped with a Photometrics Quantix CCD camera. Images were acquired with IPlab Spectrum software (Signal Analytics Corporation).

Structure-Specific DNA Substrates

X12, PX12, and Y12 were made by annealing two or more of the following PAGE purified oligonucleotides: X1 (5′-GACGCTGCCGA ATTCTGGCTTGCTAGGACATCTTTGCCCACGTTGACCCG), X2 (5′-CGGGTCAACGTGGGCAAAGATGTCCTAGCAATGTAATCGTCT ATGACGTC), X3 (5′-GACGTCATAGACGATTACATTGCTAGGACAT GCTGTCTAGAGACTATCGC), and X4 (5′-GCGATAGTCTCTAGACA GCATGTCCTAGCAAGCCAGAATTCGGCAGCGTC). DNA substrates were made by annealing a 5′-^{32}P-labeled oligonucleotide with a 5-fold excess of cold oligonucleotides. Y12-1 consists of labeled oligonucleotide X1 and cold oligonucleotide X4. PX12-1 contains labeled oligonucleotide X1 and cold oligonucleotides 2 and 4. The four different X-structures, X12-1, X12-2, X12-3, and X12-4, were made by annealing 5′-^{32}P-labeled oligonucleotide X1, X2, X3, or X4, respectively, with the other three cold oligonucleotides. X12 and PX12 contains a 12 base pair central core of homology in which the junction point is free to branch migrate. The junction is fixed in Y12. X0 was made by annealing oligonucleotides X01 (5′-CAACGTCATA GACGATTACATTGCTACATGGAGCTGTCTAGAGGATCCGA), X02 (5′-G T C G G A T CCTCTAGACAGCTCCATGATCACTGGCACTGGTA GAATTCGGC), X03 (5′-TGCCGAATTCTACCAGTGCCAGTGATGGA CATCTTTGCCCACGTTGACCC), and X04 (5′-TGGGTCAACGTGGGC AAAGATGTCCTAGCAATGTAATCGTCTATGACGTT). The annealing and gel purification of the substrates were carried out as previously described (Parsons et al., 1990). Annealing was achieved by incubating oligonucleotides for 3 min at 95°C, followed by subsequent 10 min incubations at 65°C, 37°C, room temperature, and 0°C. Labeled substrates were purified after separation by electrophoresis in a nondenaturing 10% polyacrylamide gel and stored in a TE (pH = 7.5), 50 mM NaCl buffer.

Nuclease and Resolution Assays

Cells were broken in buffer A with a Retsch mechanical grinder in the presence of liquid nitrogen. Mus81-TAP was purified from the clarified lysate as described above. TEV-eluates were stored at −80°C in 15% glycerol. Unless otherwise indicated, reactions (15 μl) contained 1 nM labeled substrate, a total of 6 μl of TEV-eluate and TEV-eluate buffer containing 15% glycerol (usually 3 μl of TEV-eluate and 3 μl of TEV-eluate buffer), 2.5 mM $MgCl_2$, 50 mM Tris pH = 7.5, 100 μg/ml BSA, and 1 mM β-Mercaptoethanol. In reactions containing ATP (2 mM), the chelation of Mg^{2+} ions by ATP was taken into account to adjust the final concentration of free Mg^{2+} ions at 2.5 mM. Reactions were incubated at 30°C for 45 min (unless otherwise indicated). Reaction products were analyzed by electrophoresis in 1X TBE in either a denaturing 12% polyacrylamide gel containing 7 M urea for nuclease assays or in a nondenaturing 10% polyacrylamide gel for resolution assays. To map the sites of cleavage in the nuclease assays, Maxam-Gilbert piperidine and hydrazine sequencing reactions set up with each oligonucleotide were run in parallel (Maxam and Gilbert, 1980).

Acknowledgments

We thank S. Saitoh for help with the TAP system, A. Constantinou for advice on preparation of DNA substrates, G. Smith and A. Toukdarian for strains, C. McGowan, X. Chen, G. Smith, and W. Heyer for helpful discussions, and members of the Scripps Cell Cycle Groups for encouragement. M.N.B. is a Research Special Fellow of the Leukemia & Lymphoma Society. W.H.M is supported by MERK-MGRI-241. J.R.Y. is supported by RO1 EY1328801, MERK-MGRI-241, and CA81665 RR11823. This work was funded by NIH grants awarded to P.R.

Received July 30, 2001; revised October 4, 2001.

References

Aravind, L., Walker, R.W., and Koonin, E.V. (1999). Conserved domains in DNA repair proteins and evolution of repair systems. Nucleic Acids Res. *27*, 1223–1242.

Bahler, J., Wu, J., Longtine, M.S., Shah, N.G., McKenzie, A., Steever, A.B., Wach, A., Phileppsen, P., and Pringle, J.R. (1998). Heterologous modules for efficient and versatile PCR-based gene targeting in *Schizosaccharomyces pombe*. Yeast *14*, 943–951.

Bardwell, A.J., Bardwell, L., Johnson, D.K., and Friedberg, E.C. (1993). Yeast DNA recombination and repair proteins Rad1 and Rad10 constitute a complex in vivo mediated by localized hydrophobic domains. Mol. Microbiol. *8*, 1177–1188.

Benard, M., Maric, C., and Pierron, G. (2001). DNA replication-dependent formation of joint DNA molecules in Physarum polycephalum. Mol. Cell *7*, 971–980.

Bennett, R.J., Dunderdale, H.J., and West, S.C. (1993). Resolution of Holliday junctions by RuvC resolvase: cleavage specificity and DNA distortion. Cell *74*, 1021–1031.

Boddy, M.N., Lopez-Girona, A., Shanahan, P., Interthal, H., Heyer, W.D., and Russell, P. (2000). Damage tolerance protein Mus81 associates with the FHA1 domain of checkpoint kinase Cds1. Mol. Cell. Biol. *20*, 8758–8766.

Carr, A.M., Schmidt, H., Kirchhoff, S., Muriel, W.J., Sheldrick, K.S., Griffiths, D.J., Basmacioglu, C.N., Subramani, S., Clegg, M., Nasim, A., et al. (1994). The rad16 gene of Schizosaccharomyces pombe: a homolog of the RAD1 gene of Saccharomyces cerevisiae. Mol. Cell. Biol. *14*, 2029–2040.

Chen, X.-B., Melchionna, R., Denis, C.-M., Gaillard, P.-H.L., Blasina, A., Van de Weyer, I., Boddy, M.N., Russell, P., Vailard, J., and McGowan, C.H. (2001). Human Mus81-associated endonuclease cleaves Holliday junctions in vivo. Mol. Cell *8*. Published online Oct. 12, 2001. 10.1016/S109727650100363x.

Collins, I., and Newlon, C.S. (1994). Meiosis-specific formation of joint DNA molecules containing sequences from homologous chromosomes. Cell *76*, 65–75.

Constantinou, A., Tarsounas, M., Karow, J.K., Brosh, R.M., Bohr, V.A., Hickson, I.D., and West, S.C. (2000). Werner's syndrome protein (WRN) migrates Holliday junctions and co-localizes with RPA upon replication arrest. EMBO Rep. *1*, 80–84.

Constantinou, A., Davies, A.A., and West, S.C. (2001). Branch migration and Holliday junction resolution catalyzed by activities from mammalian cells. Cell *104*, 259–268.

Davies, A.A., Friedberg, E.C., Tomkinson, A.E., Wood, R.D., and West, S.C. (1995). Role of the Rad1 and Rad10 proteins in nucleotide excision repair and recombination. J. Biol. Chem. *270*, 24638–24641.

de Laat, W.L., Sijbers, A.M., Odijk, H., Jaspers, N.G., and Hoeijmakers, J.H. (1998). Mapping of interaction domains between human repair proteins ERCC1 and XPF. Nucleic Acids Res. *26*, 4146–4152.

Doe, C.L., Dixon, J., Osman, F., and Whitby, M.C. (2000). Partial suppression of the fission yeast *rqh1*$^-$ phenotype by expression of a bacterial Holliday junction resolvase. EMBO J. *19*, 2751–2762.

Egel, R., and Egel-Mitani, M. (1974). Premeiotic DNA synthesis in fission yeast. Exp. Cell Res. *88*, 127–134.

Evans, E., Moggs, J.G., Hwang, J.R., Egly, J.M., and Wood, R.D. (1997). Mechanism of open complex and dual incision formation by human nucleotide excision repair factors. EMBO J. *16*, 6559–6573.

Harper, J.W., Adami, G.R., Wei, N., Keyomarsi, K., and Elledge, S.J. (1993). The p21 Cdk-interacting protein Cip1 is a potent inhibitor of G1 cyclin-dependent kinases. Cell *75*, 805–816.

Higgins, D.R., Prakash, S., Reynolds, P., and Prakash, L. (1983). Molecular cloning and characterization of the RAD1 gene of Saccharomyces cerevisiae. Gene *26*, 119–126.

Holliday, R.A. (1964). A mechanism for gene conversion in fungi. Genet. Res. *5*, 282–304.

Interthal, H., and Heyer, W.D. (2000). MUS81 encodes a novel helix-hairpin-helix protein involved in the response to UV- and methylation-induced DNA damage in Saccharomyces cerevisiae. Mol. Gen. Genet. *263*, 812–827.

Karow, J.K., Constantinou, A., Li, J.L., West, S.C., and Hickson, I.D. (2000). The Bloom's syndrome gene product promotes branch migration of Holliday junctions. Proc. Natl. Acad. Sci. USA *97*, 6504–6508.

Lilley, D.M., and White, M.F. (2001). The junction-resolving enzymes. Nat. Rev. Mol. Cell Biol. *2*, 433–443.

Lin, Y., and Smith, G.R. (1994). Transient, meiosis-induced expression of the rec6 and rec12 genes of Schizosaccharomyces pombe. Genetics *136*, 769–779.

Link, A.J., Eng, J., Schieltz, D.M., Carmack, E., Mize, G.J., Morris, D.R., Garvik, B.M., and Yates, J.R., 3rd. (1999). Direct analysis of protein complexes using mass spectrometry. Nat. Biotechnol. *17*, 676–682.

Maundrell, K. (1993). Thiamine-repressible expression vectors pREP and pRIP for fission yeast. Gene *123*, 127–130.

Maxam, A.M., and Gilbert, W. (1980). Sequencing end-labeled DNA with base-specific chemical cleavages. Methods Enzymol. *65*, 499–560.

McCormack, A.L., Schieltz, D.M., Goode, B., Yang, S., Barnes, G., Drubin, D., and Yates, J.R., 3rd. (1997). Direct analysis and identification of proteins in mixtures by LC/MS/MS and database searching at the low-femtomole level. Anal. Chem. *69*, 767–776.

Moreno, S., Klar, A., and Nurse, P. (1991). Molecular genetic analysis of fission yeast *Schizosaccharomyces pombe*. Methods Enzymol. *194*, 795–823.

Mullen, J.R., Kaliraman, V., Ibrahim, S.S., and Brill, S.J. (2001). Requirement for three novel protein complexes in the absence of the Sgs1 DNA helicase in Saccharomyces cerevisiae. Genetics *157*, 103–118.

Muris, D.F., Vreeken, K., Carr, A.M., Broughton, B.C., Lehmann, A.R., Lohman, P.H., and Pastink, A. (1993). Cloning the RAD51 homologue of Schizosaccharomyces pombe. Nucleic Acids Res. *21*, 4586–4591.

Nabeshima, K., Kakihara, Y., Hiraoka, Y., and Nojima, H. (2001). A novel meiosis-specific protein of fission yeast, Meu13p, promotes homologous pairing independently of homologous recombination. EMBO J. *20*, 3871–3881.

Nakashima, N., Noguchi, E., and Nishimoto, T. (1999). Saccharomyces cerevisiae putative G protein, Gtr1p, which forms complexes with itself and a novel protein designated as Gtr2p, negatively regulates the Ran/Gsp1p G protein cycle through Gtr2p. Genetics *152*, 853–867.

Paques, F., and Haber, J.E. (1999). Multiple pathways of recombination induced by double-strand breaks in Saccharomyces cerevisiae. Microbiol. Mol. Biol. Rev. *63*, 349–404.

Parsons, C.A., Kemper, B., and West, S.C. (1990). Interaction of a four-way junction in DNA with T4 endonuclease VII. J. Biol. Chem. *265*, 9285–9289.

Rigaut, G., Shevchenko, A., Rutz, B., Wilm, M., Mann, M., and Seraphin, B. (1999). A generic protein purification method for protein complex characterization and proteome exploration. Nat. Biotechnol. *17*, 1030–1032.

Rodel, C., Jupitz, T., and Schmidt, H. (1997). Complementation of the DNA repair-deficient swi10 mutant of fission yeast by the human ERCC1 gene. Nucleic Acids Res. *25*, 2823–2827.

Schwacha, A., and Kleckner, N. (1994). Identification of joint molecules that form frequently between homologs but rarely between sister chromatids during yeast meiosis. Cell *76*, 51–63.

Seigneur, M., Bidnenko, V., Ehrlich, S.D., and Michel, B. (1998). RuvAB acts at arrested replication forks. Cell *95*, 419–430.

Sekelsky, J.J., McKim, K.S., Chin, G.M., and Hawley, R.S. (1995). The Drosophila meiotic recombination gene mei-9 encodes a homologue of the yeast excision repair protein Rad1. Genetics *141*, 619–627.

Shiozaki, K., and Russell, P. (1997). Stress-activated protein kinase pathway in cell cycle control of fission yeast. Methods Enzymol. *283*, 506–520.

Sijbers, A.M., de Laat, W.L., Ariza, R.R., Biggerstaff, M., Wei, Y.F., Moggs, J.G., Carter, K.C., Shell, B.K., Evans, E., de Jong, M.C., et al. (1996). Xeroderma pigmentosum group F caused by a defect in a structure-specific DNA repair endonuclease. Cell *86*, 811–822.

Snow, R. (1968). Recombination in ultraviolet-sensitive strains of Saccharomyces cerevisiae. Mutat. Res. *6*, 409–418.

Stewart, E., Chapman, C., Al-Khodairy, F., Carr, A., and Enoch, T. (1997). *rqh1*$^{+}$, a fission yeast gene related to the Bloom's and Werner's syndrome genes, is required for reversible S phase arrest. EMBO J. *16*, 2682–2692.

Szostak, J.W., Orr-Weaver, T.L., Rothstein, R.J., and Stahl, F.W. (1983). The double-strand-break repair model for recombination. Cell *33*, 25–35.

Washburn, M.P., Wolters, D., and Yates, J.R., 3rd (2001). Large-scale analysis of the yeast proteome by multidimensional protein identification technology. Nat. Biotechnol. *19*, 242–247.

West, S.C. (1995). Holliday junctions cleaved by Rad1? Nature *373*, 27–28.

Zenvirth, D., and Simchen, G. (2000). Meiotic double-strand breaks in Schizosaccharomyces pombe. Curr. Genet. *38*, 33–38.

Zou, H., and Rothstein, R. (1997). Holliday junctions accumulate in replication mutants via a RecA homolog-independent mechanism. Cell *90*, 87–96.